DISTURBED STRESS FIELD MODEL FOR REINFORCED CONCRETE: FORMULATION

By F. J. Vecchio[1]

ABSTRACT: A conceptual model is presented for describing the behavior of cracked reinforced concrete elements, representing a hybrid formulation between a fully rotating crack model and a fixed crack model. The formulation described builds on the concepts of the modified compression field theory, treating cracked concrete as an orthotropic material with unique stress-strain relationships in compression and tension. Advancements in the formulation, relative to the modified compression field theory, include a new approach to the reorientation of concrete stress and strain fields, removing the restriction that they be coincident, and an improved treatment of shear stresses on crack surfaces. New sets of equilibrium, compatibility, and constitutive relations are formulated accordingly, and alternative crack slip models are discussed. The proposed theory is shown to yield improved simulations of response in specific situations where the previous formulation was found to produce inaccuracies. This paper describes the formulation of the theory at the fundamental level.

INTRODUCTION

In finite-element analysis of reinforced concrete, the development of nonlinear elastic procedures has generally progressed along two lines: rotating crack models and fixed crack models. With rotating crack models, it is assumed that a gradual reorientation occurs in the direction of cracks, as dictated by the loading or material response. Along with the change in crack direction, a gradual reorientation is assumed to occur in the principal stress and principal strain directions in the concrete. Examples of such formulations are those by Foster (1992), Ayoub and Filippou (1998), and Barzegar-Jamshidi and Schnobrich (1986). Conversely, with fixed crack models, crack directions remain fixed in the direction of first cracking. In some formulations, if the stress conditions dictate, discrete new cracks may form at alternate inclinations. An important aspect of the fixed crack approach is the determination of the shear stresses that necessarily develop on crack surfaces and the shear slips that occur as a result. Fixed crack models have been proposed by Okamura and Maekawa (1991), Kaufmann and Marti (1998), and others. Both the rotating crack and the fixed crack models have met with varying degrees of success.

The modified compression field theory (MCFT) was proposed about 20 years ago to describe the behavior of cracked reinforced concrete elements subjected to in-plane forces (Vecchio and Collins 1982, 1986). It was essentially a fully rotating, smeared crack model that represented concrete as an orthotropic material. Equilibrium, compatibility, and stress-strain relationships were formulated in terms of average stresses and average strains; however, also central to the theory was the consideration given to local stress conditions at crack locations.

In the MCFT formulation, cracked reinforced concrete was treated as distinctly different from plain uncracked concrete, with new constitutive relations derived from a comprehensive series of panel element tests. The proposed compression softening relationship reflected the observation that cracked concrete, when simultaneously subjected to high tensile strains in the direction normal to the compression, exhibited reduced strength and stiffness relative to uncracked uniaxially compressed concrete. Additionally, a tension stiffening formulation was proposed to represent the presence and influence of the postcracking average tensile stresses in the concrete between the cracks.

Subsequent to the formulation of the basic theory, work was undertaken to implement MCFT into various design code procedures and advanced analysis tools. The general design method for shear was formulated and implemented into the Canadian Code [Canadian Standards Association (CSA) 1994]. As well, a general design method was described by Collins et al. (1996), simplifying the application of the theory to design of beam elements. Concurrently, various nonlinear finite-element procedures were developed incorporating MCFT (Vecchio et al. 1996).

Since its development, MCFT has been applied to numerous situations involving a wide range of structural types, details, and loading conditions. Subsequent tests done on the panel element tester and shell element tester, involving elements subjected to plane stress conditions, exceed 150 in number (Fig. 1). In addition, a number of test programs involving more complex structural subassemblies have been undertaken. In analyzing these test specimens, MCFT was generally found to provide consistently reliable predictions of strength, load-deformation response, and failure mode to accuracies acceptable in most engineering contexts. A summary to this effect was provided by Vecchio et al. (1996). It should also be noted that, in the 20 years since its formulation, MCFT has remained essentially unchanged.

Although the accuracy and reliability of MCFT have been generally good, experience has revealed some deficiencies in

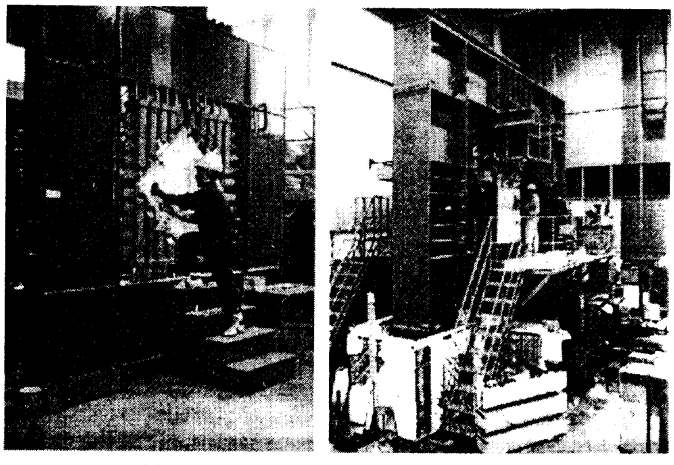

(a) (b)

FIG. 1. Testing of Panel Specimens: (a) Panel Element Tester; (b) Shell Element Tester

[1]Prof., Dept. of Civ. Engrg., Univ. of Toronto, Toronto, ON, Canada M5S 1A4.

Note. Associate Editor: Julio Ramirez. Discussion open until February 1, 2001. To extend the closing date one month, a written request must be filed with the ASCE Manager of Journals. The manuscript for this paper was submitted for review and possible publication on August 10, 1999. This paper is part of the ***Journal of Structural Engineering***, Vol. 126, No. 9, September, 2000. ©ASCE, ISSN 0733-9445/00/0009-1070–1077/$8.00 + $.50 per page. Paper No. 21621.

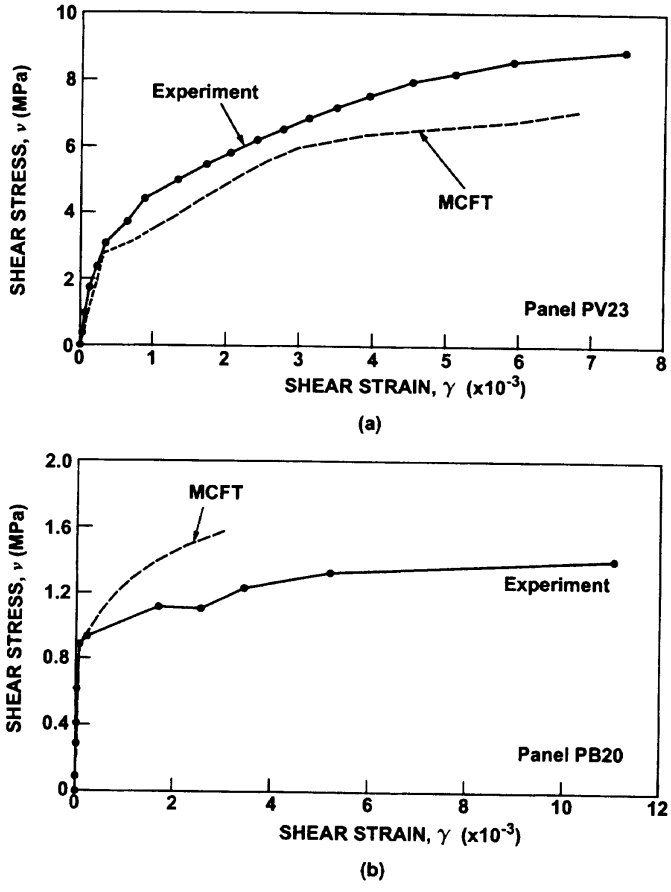

FIG. 2. Shear Stress-Strain Responses from Two Tests: (a) Panel PV23; (b) Panel PB20

specific situations. With respect to panel elements, a deterioration in accuracy is noticed under conditions as follows:

- Shear strength and stiffness are generally underestimated for panels containing heavy amounts of reinforcement in both directions, in panels subjected to high biaxial compressions in addition to shear, or in panels where the reinforcement and loading conditions are such that there is no rotation of the principal stress or strain conditions (e.g., $\rho_x = \rho_y$ and proportional loading). Shown in Fig. 2(a), for example, are the observed and computed shear responses of Panel PV23, which was reinforced with $\rho_x = \rho_y = 1.75\%$ and was subjected to biaxial compression and shear in the proportion $\sigma_x:\sigma_y:\tau = -0.32:-0.32:1$. In this panel, the degree of cracking was minimal and there was no rotation of the crack direction from the onset of cracking to the failure point. Note that the ultimate shear strength of the panel is significantly underestimated. This result is consistent with observations by Kollegger and Mehlhorn (1990) and others, who tested panels where the principal loading directions were coincident with the reinforcement directions and, hence, did not involve a reorientation of the stress-strain fields.
- Shear strength and stiffness are generally overestimated for uniaxially reinforced panels or for panels containing very light reinforcement in the transverse direction. Consider Panel PB20, tested by Bhide and Collins (1989); this panel was reinforced with $\rho_x = 1.2\%$ and $\rho_y = 0\%$ and was subjected to uniaxial tension and shear in the proportion $\sigma_x:\sigma_y:\tau = 2:0:1$. As seen in Fig. 2(b), the observed postcracking strength and stiffness are measurably less than predicted. In such panels, significant orientation of the stress-strain fields and crack directions was observed along with visible signs of slipping and crushing along the crack surfaces.

Reduced accuracy also has been observed in shear-critical beams containing very little or no transverse reinforcement (i.e., <0.05%). Here, the fully rotating crack model imbedded in MCFT allows for a significant orientation of the stress-strain fields. In such beams, this may result in overestimated ductility, and overpredicted or underpredicted strengths, depending on the structural and loading details. [It was shown that imposing two additional limit conditions on the MCFT formulations improves the accuracy of the modeling under these circumstances (Vecchio 2000).]

An original simplifying assumption of MCFT was that the directions of the average principal strain remained coincident with the directions of the average principal stresses in the concrete. The data from the initial test series clearly showed that this was strictly not the case [Fig. 3(a); note that $\theta = 90° - \psi$]. The observed tendency was for the change in the principal stress direction to lag behind the change in the principal strain direction. Shown in Fig. 3(b) are the angles of inclination for the stress and strain fields for Panel PV19, reinforced with $\rho_x = 1.8\%$ and $\rho_y = 0.7\%$ and subjected to pure shear ($\sigma_x:\sigma_y:\tau =$

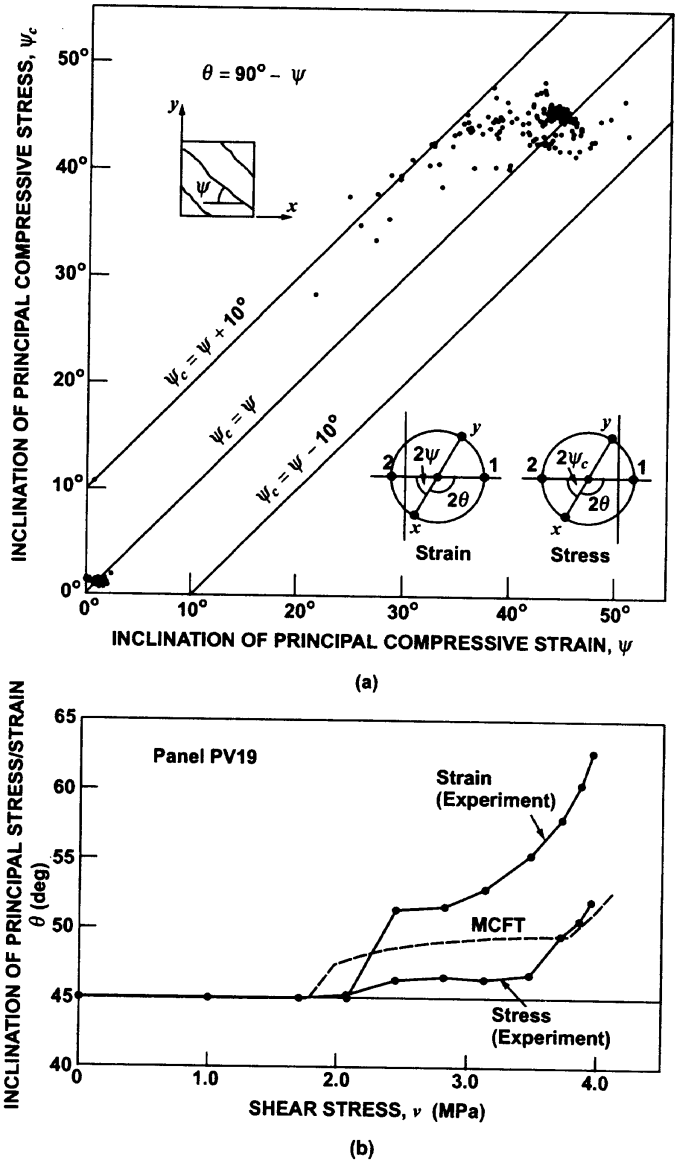

FIG. 3. Deviation of Principal Stress and Principal Strain Direction: (a) Data Reported with Original Formulation of MCFT (Vecchio and Collins 1982); (b) Results for Panel PV19

0:0:1). Prior to cracking, both fields were inclined at 45° relative to the reinforcement directions. After first cracking, there was an abrupt increase in the inclination of the principal strain direction but little change in the concrete stress field direction. Thereafter, both inclinations gradually increased, with a relatively constant differential (lag) present. After yielding of the transverse reinforcement, the reorientation of the stress field accelerated in accordance with the pattern of the change in the principal strain direction. This behavior was observed in most of the other test panels. Given that the pattern was one where the reorientation of directions of stress and strain seemed to be linked and not much different and given the significant simplification it added to the computational aspects of the theory, it was decided to make the assumption of coaxiality of stresses and strains. It is this assumption that, in large part, gives rise to the inaccuracies of MCFT for situations noted previously.

Another difficulty of MCFT, as originally constituted, stems from the crack shear check. The cracks in the concrete are assumed to align with the average principal stress directions; hence, the average shear stresses in the directions orthogonal to the crack are necessarily zero. However, at the crack surface, local stress conditions are different and can give rise to nonzero shear stresses on the crack surface (Vecchio and Collins 1986). The MCFT checks the magnitude of these local stresses; if they exceed a limit value, a reduction is made to the magnitude of the postcracking average tensile stresses that can be sustained. In reality, the relationship between the concrete tensile stresses and local shear stresses is not a direct one. Further, although shear stresses may be induced on the crack surface, the MCFT compatibility relations make no allowance for actual shear slip along the crack. Last, the crack shear check represents computational complexity that is disparate relative to the simplicity of the remainder of the formulation. The crack shear check has been the one aspect of the theory least well understood by others and often has been ignored in their implementations of MCFT, although it is a relatively important component of the model.

The disturbed stress field model (DSFM), proposed in this paper, attempts to redress the two main weaknesses in the MCFT computational model: the enforced alignment of principal stress and strain directions, and the handling of crack shear stresses. It will be shown that a more comprehensive consideration of these mechanisms helps reduce the systematic inaccuracies found in MCFT under specific circumstances. However, it also will be shown that MCFT remains a simple but powerful computational model that is applicable with sufficiently good accuracy in most practical situations.

OVERVIEW AND CONCEPTUAL MODEL

Consider a reinforced concrete structural element that has sustained cracking as a result of externally applied loads. The shear wall depicted in Fig. 4 will be used for illustrative purposes. In such elements, load is carried through the structure by internal stress fields in the concrete and by strut or tie forces in the reinforcement. In the concrete, both compression stress fields and tension stress fields typically contribute to the load resisting mechanism.

Narrowing the focus to a smaller region of the wall, consider an area spanning several cracks but one where the sectional forces can be considered relatively constant. In Fig. 4, this region corresponds to the Section 1-1 with Points A and B located at cracks. (Note that the orientation of the section line is taken normal to the crack direction.) Consider the variation of stresses that might occur over this distance (also shown in Fig. 4). The concrete tensile stresses f_{c1} will approach zero at the crack locations but will be greater than zero between the cracks due to tension stiffening and other mecha-

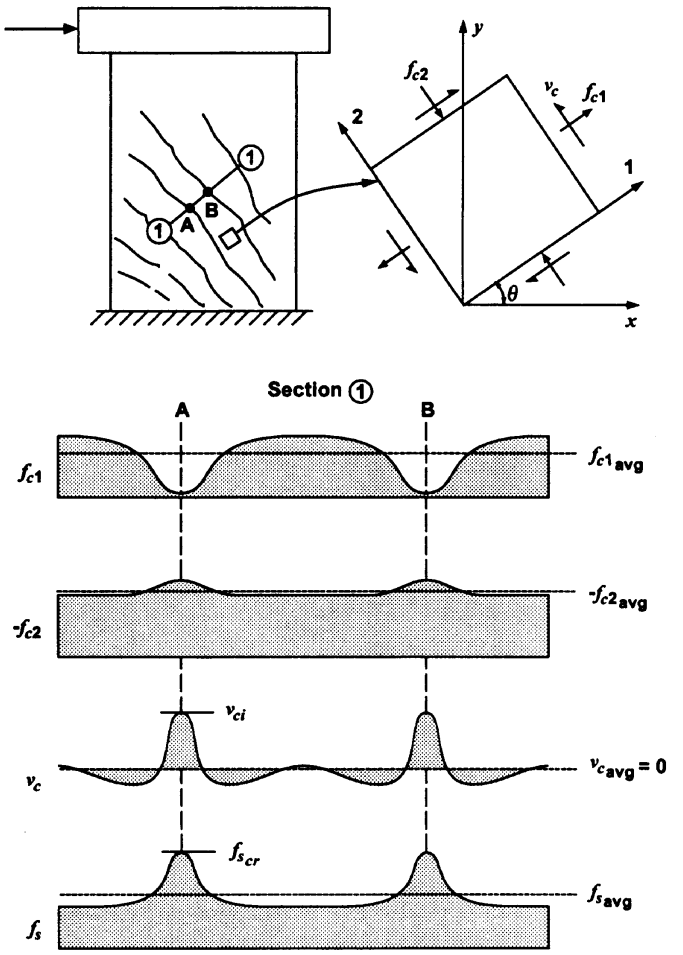

FIG. 4. Nature of Disturbed Stress Fields in Cracked Reinforced Concrete

nisms. Compensating for the reduced concrete tensile stresses at the cracks, the stresses in the reinforcement f_s increase locally to maintain force equilibrium. If the reinforcement crosses the crack at a skew angle, the locally increased reinforcement stresses will give rise to shear stresses on the crack surface v_c, as will be discussed later. However, because 1-2 reference axis represents the orientation of the concrete average principal stresses, the average concrete shear stress will necessarily be zero. Finally, the concrete compressive stresses f_{c2} will be increased somewhat near cracks due to aggregate interlock mechanisms and equilibrium requirements. Hence, it is convenient to regard the internal force resisting mechanism in terms of average stress fields but while recognizing that these fields are disturbed by the presence of cracks.

With nonzero local shear stresses present at the crack interface, a certain degree of rigid body shear slip will occur along the crack. This localized deformation must be considered in addition to the average (smeared) strains resulting from the constitutive response of the concrete to the average stresses. As will be shown, the inclusion of the slip deformations results in a deviation between the orientation of the concrete average principal stresses and that of the apparent concrete average principal strains.

A viable analytical model can be constructed by combining the local and average behaviors through the development of appropriate equilibrium, compatibility, and constitutive relations. The formulation of DSFM will proceed accordingly.

EQUILIBRIUM CONDITIONS

Fig. 5(a) shows a reinforced concrete element subjected to uniform stresses, $[\sigma] = \{\sigma_x\ \sigma_y\ \tau_{xy}\}$, applied along the element

boundaries. The element is reinforced with any number of reinforcement components oriented at arbitrary angles to the element reference axes. The reinforcement is assumed smeared and evenly distributed within the element. The problem at hand is to calculate the resulting element behavior, including load-deformation response, cracking patterns, internal stresses, and failure mode.

The forces applied to the element are resisted by internal stresses in the concrete and in the reinforcement. In this context, it is necessary to examine element equilibrium on two levels: in terms of average stresses smeared over the area of the element and in terms of local conditions along the crack surfaces.

In formulating element stiffness matrices for finite-element analysis or in developing explicit equilibrium relations for customized analysis or design procedures, it is convenient to relate average stresses to average strains. Concrete is treated as an orthotropic material with rotating cracks; hence, the concrete average principal stresses f_{c2} and f_{c1} are parallel and perpendicular, respectively, to crack direction defined by the angle θ in Fig. 6(a). Note that the average principal tensile stress f_{c1} is assumed to be present even after cracking, owing to tension softening and tension stiffening mechanisms. Average stresses also can be considered acting in the reinforcement; for the ith reinforcement component, the average stress is denoted as f_{si}. These average stress conditions are represented in Figs. 6(b and c). However, it should be noted that they do not represent conditions at any one point but rather average smeared conditions. Hence the element equilibrium condition becomes

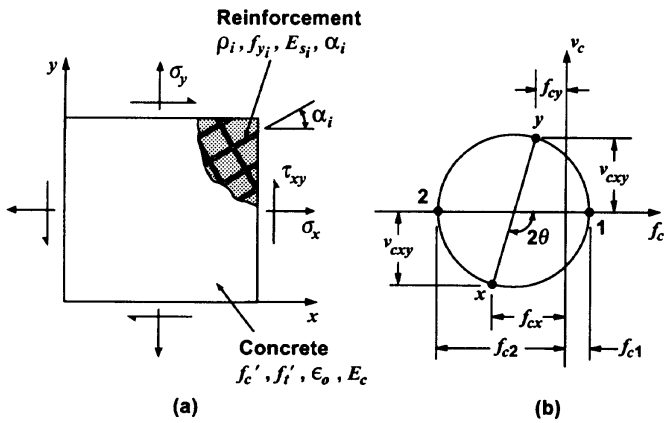

FIG. 5. Reinforced Concrete Element: (a) Reinforcement and Loading Conditions; (b) Mohr's Circle for Average Stresses in Concrete

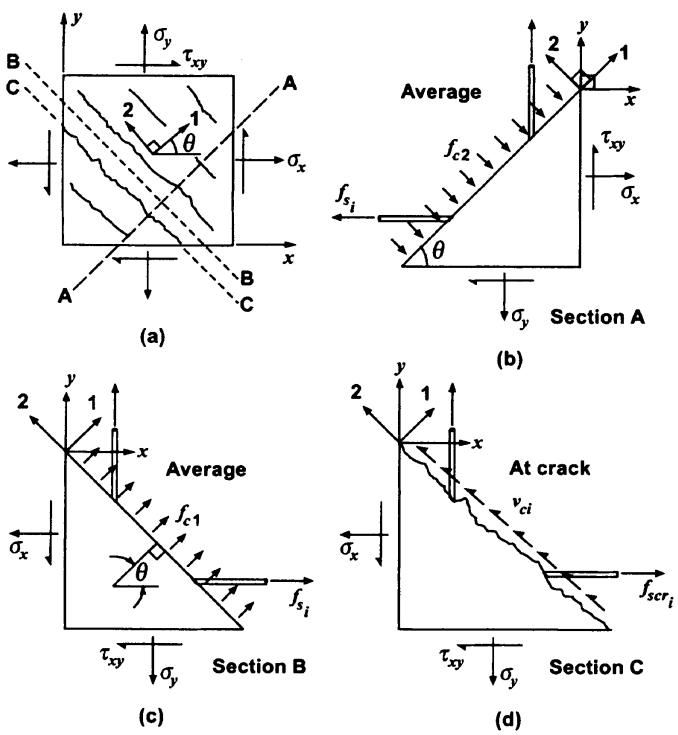

FIG. 6. Equilibrium Conditions: (a) External Conditions; (b) Perpendicular to Crack Direction; (c) Parallel to Crack Direction; (d) Along Crack Surface

$$[\sigma] = [D_c][\varepsilon_c] + \sum_{i=1}^{n} [D_s]_i[\varepsilon_s]_i \tag{1}$$

where n = number of reinforcement components; and $[D_c]$ and $[D_s]_i$ = concrete and reinforcement stiffness matrices, respectively; and $[\varepsilon_c]$ and $[\varepsilon_s]_i$ = net strains in the concrete and reinforcement components, respectively. For the special case where the panel is orthogonally reinforced and the reinforcement is aligned with the reference axes, the equilibrium equations become

$$\sigma_x = f_{cx} + \rho_x \cdot f_{sx} \tag{2}$$

$$\sigma_y = f_{cy} + \rho_y \cdot f_{sy} \tag{3}$$

$$\tau_{xy} = v_{cxy} \tag{4}$$

The concrete stresses f_{cx}, f_{cy}, and v_{cxy} can be conveniently determined from the principal stresses using the Mohr's circle of stress shown in Fig. 5(b).

Crack interfaces can be considered planes of weakness in the continuum, and it is necessary to check that the average stresses can be transmitted across the cracks. It will be assumed that the component of the concrete principal tensile stresses due to tension stiffening is zero at the crack location. To transmit the average stress f_{c1}, local increases in the reinforcement stresses are necessary. These local stresses are denoted as f_{scr_i}, as shown in Fig. 6(d). The magnitude of f_{c1} that can be transmitted via this mechanism is limited by the reserve capacity of the reinforcement, which is given by the difference between the average stresses and the yield stresses. Hence

$$f_{c1} \le \sum_{i=1}^{n} \rho_i(f_{y_i} - f_{s_i}) \cdot \cos^2\theta_{n_i} \tag{5}$$

where ρ_i = reinforcement ratio; f_{s_i} = average stress; f_{y_i} = yield stress for the ith reinforcement component; and the angle θ_{n_i} = difference between the angle of orientation of the reinforcement, α_i, and the normal to the crack surface θ:

$$\theta_{n_i} = \theta - \alpha_i \tag{6}$$

Local reinforcement stresses f_{scr_i} are determined from local reinforcement strains ε_{scr_i} (calculation of the latter are discussed in the following section). These local reinforcement stresses must satisfy the equilibrium condition that the average concrete tensile stresses be transmissible across the cracks; that is

$$\sum_{i=1}^{n} \rho_i(f_{scr_i} - f_{s_i})\cos^2\theta_{n_i} = f_{c1} \tag{7}$$

The local increases in reinforcement stresses, at crack locations, lead to the development of shear stresses along the crack surfaces v_{ci}. Equilibrium requirements produce the following relationship:

$$v_{ci} = \sum_{i=1}^{n} \rho_i(f_{scr_i} - f_{s_i})\cos\theta_{n_i} \cdot \sin\theta_{n_i} \tag{8}$$

COMPATIBILITY RELATIONS

Consider the compatibility conditions in a reinforced concrete element that is experiencing deformations composed of both continuum straining and discontinuous slip along crack surfaces. Such an element is depicted in Fig. 7. The continuum straining is the result of mechanical compliance to stress and to the smearing of crack widths over a finite area. The slip component is the result of rigid body movement along a crack interface. Using extensometers of a gauge length sufficient to span several cracks, one could make a measure of the average strains within the element. Relative to a reference x,y-system, the measured strains would intrinsically contain both components of deformation. These measured (total) or "apparent" strains will be denoted as $[\varepsilon] = \{\varepsilon_x\ \varepsilon_y\ \gamma_{xy}\}$. The apparent inclination of the principal strains θ_ε will thus be calculated

$$\theta_\varepsilon = \frac{1}{2}\tan^{-1}\left[\frac{\gamma_{xy}}{\varepsilon_x - \varepsilon_y}\right] \tag{9}$$

Decoupling the two strain effects, the actual (net) strains within the continuum will be denoted as $[\varepsilon_c] = \{\varepsilon_{cx}\ \varepsilon_{cy}\ \gamma_{cxy}\}$. It is these strains, shown in Fig. 7(a), that are to be employed in appropriate constitutive relations to determine the average stresses from the average strains for the concrete. For this purpose, the principal strains are determined from the net strains by using the standard transformations

$$\varepsilon_{c1},\ \varepsilon_{c2} = \frac{(\varepsilon_{cx} + \varepsilon_{cy})}{2} \pm \frac{1}{2}[(\varepsilon_{cx} - \varepsilon_{cy})^2 + \gamma_{cxy}^2]^{1/2} \tag{10}$$

The actual inclination of the principal strains in the continuum θ and the assumed inclination of the principal stresses θ_σ will be

$$\theta_\sigma = \theta = \frac{1}{2}\tan^{-1}\left[\frac{\gamma_{cxy}}{\varepsilon_{cx} - \varepsilon_{cy}}\right] \tag{11}$$

Consider next the discrete slip occurring along the crack surfaces [Fig. 7(b)]. Assume that the cracks are inclined in the direction of the net principal tensile strain θ, that the cracks have an average width and spacing of w and s, respectively, and that the slip along the crack surface is of magnitude δ_s. One can define an average shear slip strain as follows:

$$\gamma_s = \frac{\delta_s}{s} \tag{12}$$

Using a Mohr's circle construction, the slip strain can be resolved into orthogonal components relative to the reference system; thus $[\varepsilon^s] = \{\varepsilon_x^s\ \varepsilon_y^s\ \gamma_{xy}^s\}$ where

$$\varepsilon_x^s = -\gamma_s/2 \cdot \sin(2\theta) \tag{13}$$

$$\varepsilon_y^s = \gamma_s/2 \cdot \sin(2\theta) \tag{14}$$

$$\gamma_{xy}^s = \gamma_s \cdot \cos(2\theta) \tag{15}$$

In addition, the element may have experienced strains due to elastic or plastic offsets. The elastic strain offsets $[\varepsilon_c^0]$ will include effects due to thermal expansion, mechanical expansion (e.g., Poisson's effect and aggregate alkali reactivity), and shrinkage. Plastic offsets $[\varepsilon_c^p]$ will arise from cyclic loading conditions or loading into postpeak levels. The apparent (total) strains will be the summation of the continuum stress-induced strains, the shear slip strains, and the elastic and plastic offset strains. Hence, one obtains the following compatibility condition:

$$[\varepsilon] = [\varepsilon_c] + [\varepsilon^s] + [\varepsilon_c^0] + [\varepsilon_c^p] \tag{16}$$

For the purposes of this paper, the elastic and plastic offsets will be taken as zero. Rigorous consideration of the offset strains are easily handled in the manner described by Vecchio (1992).

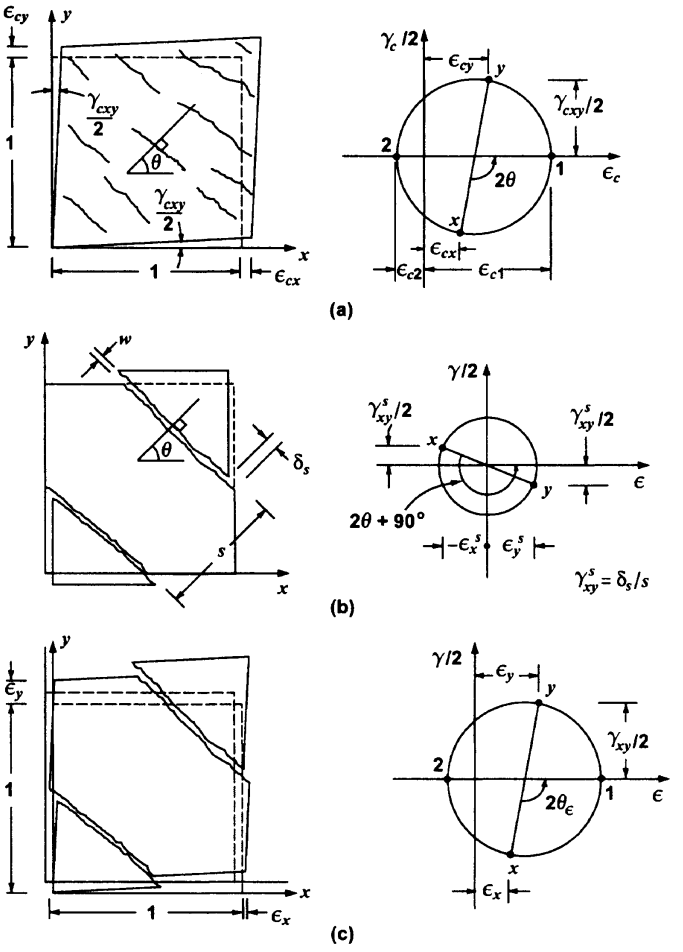

FIG. 7. Compatibility Conditions: (a) Deformations due to Average (Smeared) Constitutive Response; (b) Deformations due to Local Rigid Body Slip along Crack; (c) Combined Deformations

The "lag" in the rotation of the principal stresses in the continuum, relative to the rotation of the apparent principal strains, will be defined

$$\Delta\theta = \theta_\varepsilon - \theta_\sigma \tag{17}$$

In relating the apparent strain condition to the actual orientation of the stress and strain field within the continuum, the following relation is particularly useful:

$$\gamma_s = \gamma_{xy} \cdot \cos 2\theta_\sigma + (\varepsilon_y - \varepsilon_x) \cdot \sin 2\theta_\sigma \tag{18}$$

The reinforcement is assumed perfectly bonded to the concrete. Hence, the average strain in a reinforcement component is calculated from the total strains as follows:

$$\varepsilon_{s_i} = \frac{\varepsilon_x + \varepsilon_y}{2} + \frac{\varepsilon_x - \varepsilon_y}{2} \cdot \cos 2\alpha_i + \frac{\gamma_{xy}}{2} \sin 2\alpha_i + \varepsilon_{s_i}^0 \tag{19}$$

where α_i = angle of orientation of the reinforcement; and $\varepsilon_{s_i}^0$ = initial prestrain in the reinforcement. At crack locations, the local stresses and strains in the reinforcement must increase to compensate for the local reduction in the concrete average tensile stress. It is assumed that a local incremental strain $\Delta\varepsilon_{1cr}$ occurs in the principal stress direction such as to satisfy the equilibrium condition represented by (7). The local strain in the reinforcement will thus be

$$\varepsilon_{scr_i} = \varepsilon_{s_i} + \Delta\varepsilon_{1cr} \cdot \cos^2\theta_{n_i} \tag{20}$$

Given nominal crack spacings in the reference x- and y-directions, s_x and s_y, the average crack spacing in the cracked continuum can be estimated

$$s = \frac{1}{\frac{\sin\theta}{s_x} + \frac{\cos\theta}{s_y}} \tag{21}$$

The values s_x and s_y can be estimated from standard crack spacing formulations. From the average crack spacing, the average crack width w can then be calculated from the average tensile strain as follows:

$$w = \varepsilon_{c1} \cdot s \tag{22}$$

CONSTITUTIVE RELATIONS

The compression response of cracked reinforced concrete is characterized by significant degrees of softening arising from the effects of transverse cracking, as shown by Vecchio and Collins (1986). The principal compressive stress in the concrete f_{c2} is found to be a function of not only the principal compressive strain, but also of the coexisting principal tensile strain. This influence is captured by the reduction factor β_d, as follows:

$$\beta_d = \frac{1}{1 + C_s \cdot C_d} \leq 1.0 \tag{23}$$

In examining data collected from over 150 test panels (Vecchio and Collins 1993), the best correlations were obtained when the factor C_d was made a function of the ratio $\varepsilon_{c1}/\varepsilon_{c2}$, as follows:

$$C_d = 0.35(-\varepsilon_{c1}/\varepsilon_{c2} - 0.28)^{0.8} \tag{24}$$

The above is the preferred form for use in finite-element formulations. However, for easier implementation into design procedures, accuracy is not much reduced when using a simpler form that is a function of ε_{c1} only. In updating the MCFT formulation, the following was proposed:

$$C_d = 0.27(\varepsilon_{c1}/\varepsilon_0 - 0.37) \tag{25}$$

The factor C_s accounts for the influence of slippage on the cracks. If slip is taken into account, then the rate of compression softening due to transverse cracking must be reduced to compensate for the greater "apparent" strains obtained. That is, slip on the cracks introduces softness into the concrete response; thus, less stiffness degradation can be attributed to the tensile strain effects. This becomes apparent when one pays closer scrutiny to the test data. Shown in Fig. 8(a) is the compression softening data from all panels tested, as previously reported (Vecchio and Collins 1993). The original formulation for the softening parameter [(23) with $C_s = 1.0$] is seen to provide excellent correlation. However, shown in Fig. 8(b) are the data for only those panels that contained equal reinforcement ($\rho_x = \rho_y$), were subjected to proportional loading, and failed by concrete shear/crushing prior to yield of reinforcement, namely, PV23, PV24, PV25, PV27, and PV28. Panels in this latter group, owing to the conditions cited, experienced no rotation of crack direction during the course of testing. It is notable and significant that the response for these panels is appreciably stiffer and stronger than that for the test panels as a whole. Examining conditions at the ultimate load stages, it is found that using $C_s = 0.55$ in (23) produces improved fit; hence, this is the value adopted for the DSFM. If slip on the cracks is not being explicitly taken into account in the element compatibility relations, as when using the MCFT formulation, then $C_s = 1.0$ is used.

The factor β_d is used to define both the peak stress f_p and

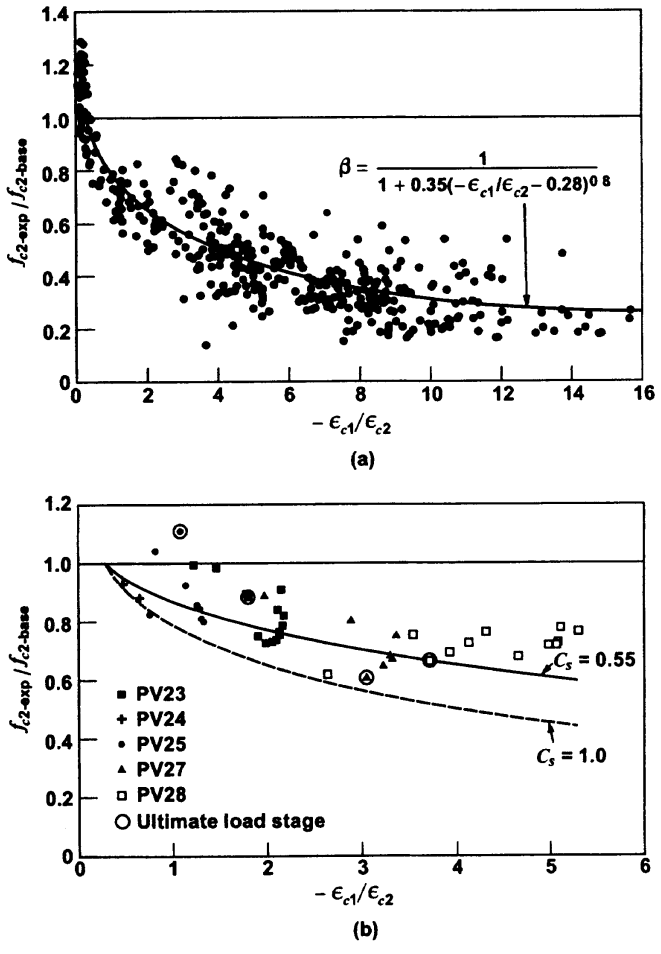

FIG. 8. Compression Softening of Cracked Concrete: (a) Data from All Test Panels (Vecchio and Collins 1993); (b) Data from Panels Experiencing No Crack Rotation

the strain at peak stress ε_p in the compression response of the concrete. Hence, if using the $\varepsilon_{c1}/\varepsilon_{c2}$ formulation, then

$$f_p = -\beta_d \cdot f'_c \tag{26}$$

$$\varepsilon_p = -\beta_d \cdot \varepsilon_0 \tag{27}$$

If using the ε_{c1} formulation, then $\varepsilon_p = -\varepsilon_0$. (Note that ε_p and f_p are negative quantities.) As previously suggested (Vecchio and Collins 1993), a suitable compression response curve is given by the following:

$$f_{c2} = f_p \cdot \frac{n \cdot (\varepsilon_{c2}/\varepsilon_p)}{(n - 1) + (\varepsilon_{c2}/\varepsilon_p)^{nk}} \tag{28}$$

where

$$n = 0.80 - f_p/17 \tag{29}$$

$$k = 1.0, \quad \varepsilon_p < \varepsilon_{c2} < 0; \quad k = (0.67 - f_p/62), \quad \varepsilon_{c2} < \varepsilon_p \tag{30a,b}$$

See Fig. 9(a); note that the compression response is assumed to decay to zero when the crack width reaches 5 mm, for reasons discussed elsewhere (Vecchio 2000).

For concrete in tension, prior to cracking, a linear relation is used; that is

$$f_{c1} = E_c \varepsilon_{c1}, \quad 0 < \varepsilon_{c1} < \varepsilon_{cr} \tag{31}$$

where E_c = initial tangent modulus of the concrete; and ε_{cr} = cracking strain. Recent experience with concrete made from Toronto-area aggregates suggest the following relationship for estimating the concrete tensile strength f'_t:

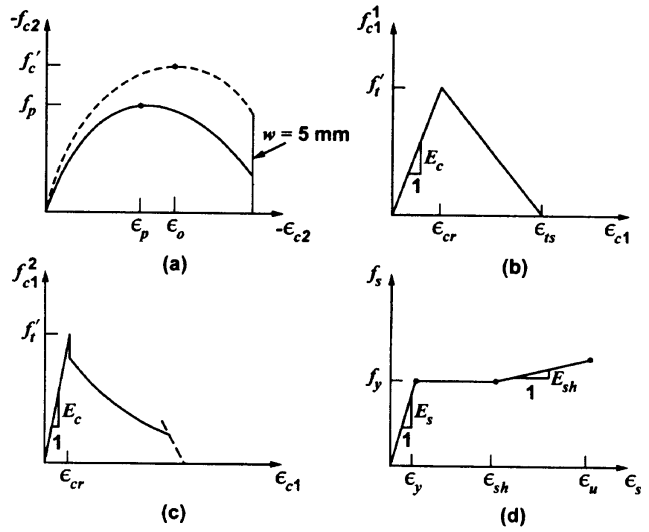

FIG. 9. Constitutive Relations: (a) Compressive Softening Model; (b) Tension Softening Model; (c) Tension Stiffening Model; (d) Reinforcing Steel Response

$$f_t' = 0.65(f_c')^{0.33} \tag{32}$$

After cracking, concrete can continue to carry tensile stresses as a result of two independent mechanisms: tension softening and tension stiffening. Tension softening refers to the fracture-associated mechanisms described by Darwin and others. It is particularly significant in concrete structures containing little or no reinforcement; for example, beams containing no web steel. Here, the concrete postcracking tensile stress associated with tension softening f_{c1}^a is calculated

$$f_{c1}^a = f_t' \left[1 - \frac{(\varepsilon_{c1} - \varepsilon_{cr})}{(\varepsilon_{ts} - \varepsilon_{cr})} \right] \tag{33}$$

where the terminal strain ε_{ts} is calculated from the fracture energy parameter G_f and characteristic length L_r as follows:

$$\varepsilon_{ts} = 2.0 \frac{G_f}{f_t' \cdot L_r} \tag{34}$$

The parameter G_f is taken as having a constant value of 75 N/m. The resulting concrete tension softening formulation is illustrated in Fig. 9(b). This linear formulation is sufficient for most applications, but more accurate nonlinear models can be used.

Postcracking tensile stresses in the concrete also arise from interactions between the reinforcement and the concrete. In areas between cracks, load is transferred from the reinforcement to the concrete via bond stresses, producing significant levels of average tensile stress in the concrete. As previously done in the MCFT, these concrete tension stiffening stresses are modeled as follows:

$$f_{c1}^b = \frac{f_t'}{1 + \sqrt{c_t \varepsilon_{c1}}} \tag{35}$$

Previously, the MCFT used $c_t = 200$ for relatively small elements or elements containing a closely spaced mesh of reinforcement and $c_t = 500$ for larger-scale elements. However, Bentz (1999) showed that the degree of tension stiffening is dependent on, among other factors, the reinforcement ratio ρ and the rebar diameter d_b; he formulated an improved relationship accordingly. Modifying the Bentz equation to account for direction-dependent behavior, the following relationship is suggested for the tension stiffening coefficient:

$$c_t = 2.2m \tag{36}$$

where

$$\frac{1}{m} = \sum_{i=1}^{n} \frac{4\rho_i}{d_{b_i}} \cdot |\cos \theta_{n_i}| \tag{37}$$

This model is illustrated in Fig. 9(c). Note that f_{c1}^b is limited to the amount that can be transmitted across cracks, as previously discussed [(5)]. The resulting average principal tensile stress in the concrete is the larger of the two values defined above. Hence

$$f_{c1} = \max(f_{c1}^a, f_{c1}^b) \tag{38}$$

A trilinear stress-strain relation is used to model the response of reinforcement in tension or compression. Hence

$$f_s = E_s \varepsilon_s, \quad 0 < \varepsilon_s < \varepsilon_y; \quad f_s = f_y, \quad \varepsilon_y < \varepsilon_s < \varepsilon_{sh} \tag{39a,b}$$

$$f_s = f_y + E_{sh}(\varepsilon_s - \varepsilon_{sh}), \quad \varepsilon_{sh} < \varepsilon_s < \varepsilon_u; \quad f_s = 0, \quad \varepsilon_s > \varepsilon_u \tag{39c,d}$$

where f_y = yield strength; E_s = modulus of elasticity; E_{sh} = strain hardening modulus; ε_y = yield strain; ε_{sh} = strain at start of strain hardening; and ε_u = ultimate strain. This formulation, illustrated in Fig. 9(d), is used for the calculation of both average and local stresses (f_{s_i} and f_{scr_i}), given the corresponding reinforcement strains (ε_{s_i} and ε_{scr_i}). The model can be modified to reflect Bauschinger effect under cyclic load conditions or to reflect curvilinear response for prestressing steel.

SLIP MODEL

Numerous studies are reported in the literature quantifying the amount of slip δ_s along a crack surface as a function of the acting shear stress v_{ci}. These formulations are typically also functions of the crack width w, aggregate size a, and concrete compressive cylinder strength f_c' or cube strength f_{cc}. The relationship adopted here is that of Walraven (1981), taking the stiffness portion of his formulation as follows:

$$\delta_s^a = \frac{v_{ci}}{1.8w^{-0.8} + (0.234w^{-0.707} - 0.20) \cdot f_{cc}} \tag{40}$$

Once the slip displacement δ_s^a has been found, (12) is used to determine the crack slip shear strain γ_s^a.

Shear-slip models of the type above can be easily implemented into the analysis model and provide reasonably accurate simulations of response in most cases. However, there are two difficulties that arise when implemented into the analytical formulation suggested herein. First, although they correctly recognize that some initial slip is required before the gap between opposing crack surfaces is closed and traction is developed, including the initial slip component in the analysis procedure proves to be numerically problematic. Second, in the case of elements that are locally unreinforced (for example, in the web regions of beams that contain no shear reinforcement), the equilibrium equations previously presented result in a calculation of zero shear stresses on the crack surface [(8)]. That is, no account is made of the shear stresses that arise from aggregate interlock or other mechanisms. Zero shear stresses necessarily result in a calculated zero shear slip, and this is intuitively unsatisfactory.

A supplemental approach is to relate the changes in direction of the principal stresses to the changes in the direction of the apparent principal strains. As was seen in Fig. 3(b) for Panel PV19, and also observed in many other tests involving panels with reinforcement crossing the cracks at skew angles, the stress field rotation tends to lag behind the strain field rotation. This lag is established soon after first cracking and remains relatively constant in the earlier stages of loading until one of the reinforcement components begins to yield. Observations made from the test panels indicated that the initial lag

is approximately between 5° and 10°, depending on the reinforcement conditions.

Relative to the initial crack direction θ_{ic} (i.e, inclination of principal stresses/strains at first cracking), the rotation in the apparent principal strains $\Delta\theta_\varepsilon$ is determined first according to the prevailing load and material conditions at the current load state

$$\Delta\theta_\varepsilon = \theta_\varepsilon - \theta_{ic} \tag{41}$$

Allowing for the rotation lag, the change in inclination of the principal stress direction $\Delta\theta_\sigma$ can next be found

$$\Delta\theta_\sigma = (\Delta\theta_\varepsilon - \theta^\ell) \quad \text{for} \quad |\Delta\theta_\varepsilon| > \theta^\ell \tag{42a}$$

$$\Delta\theta_\sigma = \Delta\theta_\varepsilon \quad \text{for} \quad |\Delta\theta_\varepsilon| \leq \theta^\ell \tag{42b}$$

where the constant lag θ^ℓ is taken as 5° for biaxially reinforced elements, 7.5° for uniaxially reinforced elements, and 10° for reinforced elements. The inclination of the stress field at the current load stage is then calculated

$$\theta_\sigma = \theta_{ic} + \Delta\theta_\sigma \tag{43}$$

Then, using (18), the crack shear slip strain γ_s^b can be determined. The weakness in this approach, apart from being based entirely on empirical evidence and lacking some objectivity, is that at later load stages the rotation lag ceases to be relatively constant and begins to escalate.

Combining the two approaches into a hybrid formulation effectively eliminates the deficiencies of each. The crack slip shear strain can be taken as the maximum values; hence

$$\gamma_s = \max(\gamma_s^a, \gamma_s^b) \tag{44}$$

At early stages of loading or in unreinforced elements the constant rotation lag criterion will govern as the slip is largely influenced by the lateral closing of the gap across the opposing crack surfaces. At more advanced stages of loading, the explicit expression for the crack shear slip will become critical as the slip is then largely dictated by the shear stresses that develop on the crack surfaces. The hybrid approach results in a model that captures the relevant mechanisms and one that closely corresponds to observed behavior

CONCLUSIONS

The DSFM is proposed as an alternative smeared crack model for the analysis of cracked reinforced concrete. Compatibility, equilibrium, and constitutive response are formulated in terms of average stresses and average strains, with particular attention given to compression softening and tension stiffening mechanisms. However, an important aspect of the theory also is to consider the local conditions at crack locations, because the presence of cracks creates disturbances in the stress fields that can influence behavior. The key advancement in the theory is the inclusion of discrete slip on the crack surfaces in the formulation of compatibility relations.

The analytical procedure that results from the slip formulation is one that occupies a middle ground between fixed crack models and rotating crack models, capturing the strengths of each. Unlike conventional fixed crack models, the DSFM allows for a gradual and progressive reorientation of concrete principal stress direction (and crack direction), however, delayed to a certain extent. Unlike common rotating crack models, the DSFM allows for the divergence of principal stress and principal strain directions. In both respects, this is more consistent with observed behavior.

The DSFM is an extension of the MCFT. However, by explicitly including crack shear slips in the compatibility relations, the resulting improvements relative to the MCFT are

- The inclinations of the principal stresses and principal strains are no longer necessarily equal.
- Behavior and failure conditions influenced by crack shear slip are better represented.
- The troublesome check on the crack shear stress is eliminated.
- The degree of softening of the compression response, as a result of cracking per se, is substantially reduced and more consistent with that reported by others.

APPENDIX. REFERENCES

Ayoub, A., and Filippou, F. C. (1998). "Nonlinear finite element analysis of RC shear panels and walls." *J. Struct. Engrg.*, ASCE, 124(3), 298–308.

Barzegar-Jamshidi, F., and Schnobrich, W. C. (1986). "Nonlinear finite element analysis of reinforced concrete under short-term monotonic loading." *Civ. Engrg. Studies Rep. No. 530*, University of Illinois at Urbana-Champaign, Urbana, Ill.

Bentz, E. C. (1999). "Sectional analysis of reinforced concrete structures." PhD thesis, Dept. of Civ. Engrg., University of Toronto, Toronto.

Bhide, S. B., and Collins, M. P. (1989). "Influence of axial tension on the shear capacity of reinforced concrete members." *ACI Struct. J.*, 86(5), 570–581.

Canadian Standards Association (CSA) Committee A23.3. (1994). "Design of concrete structures: Structures (design)—A national standard of Canada." Rexdale, Ont., Canada.

Collins, M. P., Mitchell, D., Adebar, P., and Vecchio, F. J. (1996). "A general shear design method." *ACI Struct. J.*, 93(1), 36–45.

Foster, S. J. (1992). "The structural behavior of reinforced concrete deep beams." PhD dissertation, University of New South Wales, New South Wales, Australia.

Kaufmann, W., and Marti, P. (1998). "Structural concrete: Cracked membrane model." *J. Struct. Engrg.*, ASCE, 124(12), 1467–1475.

Kollegger, J., and Mehlhorn, G. (1990). "Experimentelle Untersuchungen zur Bestimmung der Druckfestigkeit des gerissenen Stahlbetons bei einer Querzugbeanspruchung." *Rep. 413*, Deutscher Ausschuss für Stahlbeton, Berlin.

Okamura, H., and Maekawa, K. (1991). "Nonlinear analysis and constitutive methods of reinforced concrete." *ISBN 7655-1506-0*, University of Tokyo, Tokyo.

Vecchio, F. J. (1992). "Finite element modeling of concrete expansion and confinement." *J. Struct. Engrg.*, ASCE, 118(9), 2390–2406.

Vecchio, F. J. (2000). "Analysis of shear-critical reinforced concrete beams." *ACI Struct. J.*, 97(1), 102–110.

Vecchio, F. J., and Collins, M. P. (1982). "Response of reinforced concrete to in-plane shear and normal stresses." *Rep. No. 82-03*, Dept. of Civ. Engrg., University of Toronto, Toronto.

Vecchio, F. J., and Collins, M. P. (1986). "The modified compression field theory for reinforced concrete elements subjected to shear." *ACI J.*, 83(2), 219–231.

Vecchio, F. J., and Collins, M. P. (1993). "Compression response of cracked reinforced concrete." *J. Struct. Engrg.*, ASCE, 119(12), 3590–3610.

Vecchio, F. J., Polak, M. A., and Selby, R. G. (1996). "Nonlinear analysis of reinforced concrete: The University of Toronto experience." *Proc., 3rd Asian-Pacific Conf. on Computational Mech.*

Walraven, J. C. (1981). "Fundamental analysis of aggregate interlock." *J. Struct. Engrg.*, ASCE, 107(11), 2245–2270.